Transformation of the sex pheromone signal in the noctuid moth agrotis ipsilon: From peripheral input to antennal lobe output

David D. Jarriault, Christophe C. Gadenne, Philippe P. Lucas, Jean-Pierre J.-P. Rospars, Sylvia Anton

Chem. Senses 35: 705–715, 2010

doi:10.1093/chemse/bjq069
Advance Access publication July 2, 2010

Transformation of the Sex Pheromone Signal in the Noctuid Moth *Agrotis ipsilon*: From Peripheral Input to Antennal Lobe Output

David Jarriault, Christophe Gadenne, Philippe Lucas, Jean-Pierre Rospars and Sylvia Anton

Unité Mixte de Recherches 1272 Physiologie de l'Insecte: Signalisation et Communication, Institut National de la Recherche Agronomique, Route de Saint Cyr, F-78000 Versailles, France

Correspondence to be sent to: Sylvia Anton, Unité Mixte de Recherches 1272 Physiologie de l'Insecte: Signalisation et Communication, Institut National de la Recherche Agronomique, Route de Saint-Cyr, F-78000 Versailles, France. e-mail: sylvia.anton@versailles.inra.fr

Accepted June 2, 2010

Abstract

How information is transformed along synaptic processing stages is critically important to understand the neural basis of behavior in any sensory system. In moths, males rely on sex pheromone to find their mating partner. It is essential for a male to recognize the components present in a pheromone blend, their ratio, and the temporal pattern of the signal. To examine pheromone processing mechanisms at different levels of the olfactory pathway, we performed single-cell recordings of olfactory receptor neurons (ORNs) in the antenna and intracellular recordings of central neurons in the macroglomerular complex (MGC) of the antennal lobe of sexually mature *Agrotis ipsilon* male moths, using the same pheromone stimuli, stimulation protocol, and response analyses. Detailed characteristics of the ORN and MGC-neuron responses were compared to describe the transformation of the neuronal responses that takes place in the MGC. Although the excitatory period of the response is similar in both neuron populations, the addition of an inhibitory phase following the MGC neuron excitatory phase indicates participation of local interneurons (LN), which remodel the ORN input. Moreover, MGC neurons showed a wider tuning and a higher sensitivity to single pheromone components than ORNs.

Key words: intracellular recording, macroglomerular complex, MGC neuron, olfactory coding, olfactory receptor neuron, single sensillum recording

Introduction

In both vertebrates (Buck and Axel 1991; Buck 1996) and insects (Clyne et al. 1997; Vosshall et al. 1999), each odorant receptor (OR) gene is expressed in distinct populations of olfactory receptor neurons (ORNs) of the nasal mucosa (vertebrates) or the antennal sensilla (insects). In insects, axons of ORNs expressing the same OR converge onto a single glomerulus of the antennal lobe (AL), the counterpart of the vertebrate olfactory bulb (Gao et al. 2000; Vosshall et al. 2000). Each glomerulus contains arborizations of local interneurons (LNs) confined to the AL and projection neurons (PNs) that transmit the integrated information to the next processing level in the protocerebrum (for review, see Anton and Homberg 1999). Synaptic contacts have been described between ORNs, LNs, and PNs: from ORNs to PNs (Malun 1991; Stocker 1994; Distler and Boeckh 1996) and LNs (Tolbert and Hildebrand 1981; Distler 1990), from LNs to ORNs and PNs (Distler and Boeckh 1997), and from PNs to LNs (Malun 1991).

In moths, the integration of information about pheromone components is performed in a cluster of glomeruli separated from ordinary glomeruli, called the macroglomerular complex (MGC) (for review, see Koontz and Schneider 1987; Rospars 1988; Anton and Homberg 1999). One special feature of the pheromonal system resides in the high specificity of the ORs for their ligand (Mori 1998). Each pheromone component is thus detected by a distinct functional ORN type (Krieger et al. 2002; Sakurai et al. 2004), which projects into a unique glomerulus (Hansson et al. 1992; Christensen et al. 1995a; Ochieng et al. 1995; Todd et al. 1995; Berg et al. 1998; Lee et al. 2006a,b; Karpati et al. 2008). Moreover, the converging ratio of ORNs in the MGC is very high because of a much larger number of ORNs dedicated to the detection of sex pheromone components in male moths in comparison with a smaller number of PNs arborizing in the MGC (Rospars 1988; Homberg et al. 1989; Hartlieb et al. 1997; Hansson and Christensen 1999).

In the noctuid moth *Agrotis ipsilon*, as in many other moth species, pheromone communication is crucial for mating. Males rely on the plume of pheromone emitted by conspecific females to locate them. At least the 5 following components are present in the pheromone blend: *cis*-7-dodecenyl acetate (Z7-12:Ac), *cis*-9-tetradecenyl acetate (Z9-14:Ac), *cis*-11-hexadecenyl acetate (Z11-16:Ac), *cis*-11-tetradecenyl acetate, and *cis*-11-hexadecenyl alcohol (Picimbon et al. 1997). Wind tunnel experiments showed that a blend of the main component, Z7-12:Ac, with Z9-14:Ac and Z11-16:Ac in a ratio of 4:1:4 is sufficient to elicit the full courtship behavior (Wakamura et al. 1986; Causse et al. 1988). Two categories of ORNs responding to Z7-12:Ac and Z9-14:Ac, respectively, were found in distinct sensilla of the male antenna, whereas no neurons tuned to Z11-16:Ac have been found so far (Renou et al. 1996). MGC-neuron responses to the sex pheromone have recently been quantitatively analyzed in sexually mature males, revealing homogeneous response patterns, with an inhibitory phase following excitation (Jarriault et al. 2009). Most if not all of these neurons are believed to be PNs because the stained neurons presenting this response pattern always showed morphological characteristics of PNs.

To better understand the integrative role of the AL, we studied here, with the same experimental protocol as previously used with MGC neurons (Jarriault et al. 2009), how the 3 main components of the female pheromone blend are encoded in ORNs. Then, we could compare firing activity in ORNs and MGC neurons and investigate how the qualitative, quantitative, and temporal aspects of the stimulus are transformed during integration of the ORN input signal in the MGC-neuron output signal.

Materials and methods

Animals

Agrotis ipsilon were reared in the laboratory according to a standard protocol (Poitout and Buès 1974). Larvae were kept in individual plastic cups and fed on an artificial diet. Pupae and adults were maintained at 23 ± 1 °C and 50 ± 5% relative humidity under a long-day reversed photoperiod (16:8 h light:dark). Sexes were separated at the pupal stage to prevent exposure of males to the female pheromone. Adult males and females were kept in the same conditions and fed ad libitum with a 20% sucrose solution. All experiments were performed during the scotophase on sexually mature virgin males 5 days after their adult emergence.

Stimulation

Three main components of the pheromone blend of *A. ipsilon* were used: Z7-12:Ac, Z9-14:Ac, and Z11-16:Ac (Picimbon et al. 1997; Gemeno and Haynes 1998). These compounds were diluted in hexane and applied to a filter paper at doses ranging in decadic steps from 0.01 to 100 ng. All stimuli were presented after a minimum evaporation time of 30 min. The same stimulation system was used for both single sensillum and intracellular recordings in the AL. A stimulus controller (CS 55, Syntech) delivered a constant charcoal-filtered and humidified airflow on the antenna by means of a glass tube (inner diameter 8 mm). The antenna was placed in the outlet of this glass tube. The continuous airflow velocity was 0.3 m s^{-1} (17 mL s^{-1}). Stimuli were applied by inserting a Pasteur pipette containing a filter paper, impregnated with a single pheromone component or with hexane only, in the glass tube, 20 cm upstream of the antenna. An air pulse (7 mL s^{-1}) was blown through the Pasteur pipette. The stimulus was delivered during 200 ms when testing the specificity and the dose–response relationship and during at least 3 of the following durations, 0.1, 0.2, 0.3, 0.4, 0.5, 0.6, 0.7, 0.8, 1, 1.2, 1.3, 1.5, 2 s at 10 ng dose, when testing the relationship between stimulus duration and response duration. The mechanical component of the stimulation was minimized by adding a constant airflow of the same velocity as the stimulus to the continuous airflow between stimuli. Stimuli were presented randomly, separated by interstimulus intervals of at least 10 s (1 min for single sensillum recordings), with lower stimulus loads tested first.

Electrophysiology

Single sensillum recordings

Animals were mounted in a styrofoam block holder with the head protruding. One bipectinate antenna was fixed with adhesive tape and oriented to allow an optimal access to trichoid sensilla selected randomly along the stem and branches in the middle part of the antenna (10th to 34th segments from the base). Recordings were carried out according to the tip recording technique (Kaissling and Thorson 1980). Tips of a few hairs were cutoff using sharpened forceps. Reference and recording microelectrodes were filled with saline solutions, which approximated respectively the ionic composition of the hemolymph and the sensillum lymph of moths (Kaissling and Thorson 1980). The tip of the recording microelectrode was filled with polyvinylpyrrolidon (20% in sensillum saline) to prevent exchange between sensillum lymph and electrolyte. To minimize contributions of field potentials, the reference electrode was inserted into a segment adjacent to the recording site. Recorded signals were amplified (×500), low-pass filtered at 5 kHz using an Axopatch 200B amplifier (Molecular Devices), and monitored on a computer using a Digidata 1322A acquisition board (Molecular Devices) driven by Clampex 10 software (Molecular Devices). The recorded signal was low-pass filtered offline (Gaussian, 50 Hz) using Clampfit 10, and the result was subtracted from the original trace to generate a pseudo high-pass filtering that does not distort the shape of action potentials (APs) (Dolzer et al. 2003). APs were then detected and sorted according to their amplitude and shape to keep only APs of the

responding ORN (or APs of the most easily extractable class of APs if 2 ORNs responded).

Intracellular recordings from MGC neurons

Data on MGC neurons from a previous study (Jarriault et al. 2009) were used for comparison with data on ORNs. Briefly, intracellular recordings were performed according to standard methods (Christensen and Hildebrand 1987). The tip of each glass microelectrode was filled either with Lucifer Yellow CH or with Neurobiotin. The microelectrode was located near the synaptic neuropil of the MGC, which implies that the recordings were made from primary neurites, axons, or dendrites of AL neurons in the MGC area. Neurons were identified a posteriori. After establishing intracellular contact, the activity of the neuron was monitored before, during, and after stimulation of the ipsilateral antenna.

Data analysis

Compiled data files of the recordings from single sensilla and AL neurons were exported to Matlab (The MathWorks) for analysis. The threshold, frequency, latency, and duration of the AP responses to odorant stimulations were quantified as follows and expressed as means ± standard error of the mean.

Frequency

The firing frequency was first measured as the instantaneous AP frequencies averaged in 5 APs around (2 before and 2 after) the AP with the highest instantaneous frequency (for details, see Jarriault et al. 2009). Moreover, to compare the time course of changes in firing frequency in the ORN and MGC-neuron populations in response to a pheromone stimulus, we calculated peristimulus time histograms (PSTH) by pooling trains of APs available for all neurons in each group and calculating the mean of the frequencies per 50-ms bins across all neurons. Normalized PSTHs (for ORNs and MGC neurons) shown in Figure 1 were produced first by subtracting the spontaneous activity averaged on the period of recording before the stimulus and then by dividing the frequency in each bin by the maximum frequency in the response. This measure is therefore expressed in percentage of the maximum firing frequency. PSTHs of ORNs presented in Figures 4 and 5 were smoothed for more accurate calculation of activity at the moment when MGCs ceased to fire.

Response threshold

An ORN was considered as responding when its firing frequency (calculated as above) was at least 5 APs/s higher than the spontaneous activity. For MGC neurons, the tested doses were too high to determine the response threshold directly; it was therefore estimated for each neuron from the dose–response curve (see Jarriault et al. 2009 for details). Briefly, the dose–response curve characterizing each MGC neuron was extrapolated from its linear part to the level of response to the blank. The concentration at which the firing frequency was equal to the value of the blank was considered as the response threshold.

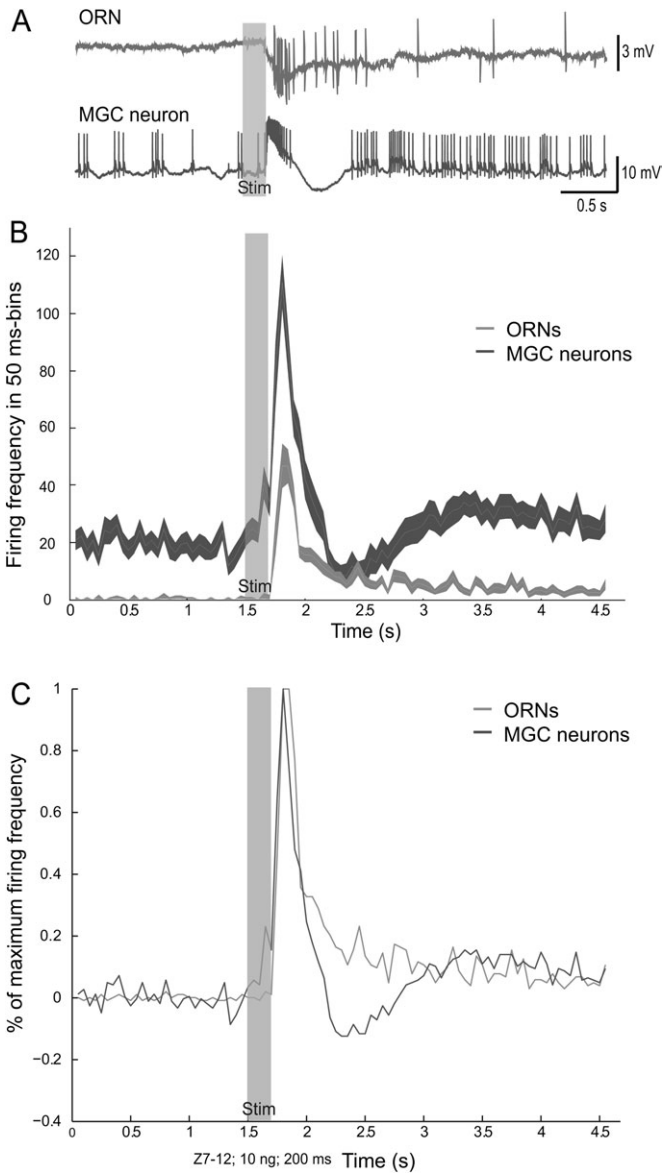

Figure 1 Response patterns of ORNs (gray) and MGC neurons (black) to the same stimulation (Z7-12:Ac; 10 ng; 200 ms). **(A)** Original recordings of the response of an ORN and an MGC neuron. **(B)** PSTH of the responses of 45 ORNs and 29 MGC neurons (bin width = 50 ms). The width of the curve represents the standard error of the mean firing frequency in each bin. The firing frequency is higher in the MGC-neuron population both without stimulation and during the excitatory phase of the response. Note that the maximum firing frequency occurs at the same time (0.3 s after the stimulus onset) for ORNs and MGC neurons. **(C)** Normalized PSTHs from (B). Spontaneous activity was subtracted from the mean firing frequency in each 50-ms bin and the values were divided by the maximum firing frequency. The ORN and MGC-neuron signals are well superimposed during the excitatory phase but not during the inhibitory phase of the MGC neurons. The gray bar represents the stimulation period (Stim).

Latency

For ORNs and MGC neurons, the latency was measured as the time elapsed from the stimulus onset to the first AP of the response.

Duration

For high doses (10 or 100 ng) the firing activity of ORNs did not return to the prestimulus level within the duration of the recording. Therefore, to evaluate the duration of the response, we used the average signal represented by the mean PSTHs of the neuron population (see *Frequency* above) and we measured the duration during which the mean firing frequency was above 10% of the maximum reached during the response. In MGC neurons, excitatory phase durations were measured from the first AP of the response to the AP just preceding the inhibitory phase.

Statistics

Dose–response relationships were tested using one-way analysis of variance (ANOVA) with repeated measures, whenever possible (equal numbers of observations).

Results

We compared response characteristics from ORNs and MGC neurons when stimulated with the same pheromone stimuli varying with respect to the compound, the stimulus load and duration. In total, 101 pheromone-responding sensilla were recorded from 48 males. After AP sorting analysis, 79 sensilla showed a unique class of AP amplitude, whereas 22 sensilla showed more than one class of APs. In the latter case, only one class of APs, that is, originating from a single responding ORN, was analyzed. Thus, ORNs used in this study originate from these 101 sensilla, and each ORN was from a different sensillum. This sample of ORNs was compared with a set of 139 MGC neurons recorded intracellularly (Jarriault et al. 2009).

Response patterns of ORNs and MGC neurons are different

When comparing responses of ORNs and MGC neurons to the same pheromone stimulation, the most obvious difference was in the temporal pattern of their AP firing rate. All ORNs showed an increase of their firing activity during a long time, that is, a long excitatory response, whereas a large majority of MGC neurons (97%) responded with an excitatory phase, which lasted approximately as long as the stimulus, followed by an inhibitory phase. The excitatory phase of the responses in both neuron types was composed of a phasic part followed by a more tonic part (Figure 1A,B and see Jarriault et al. 2009 for a more detailed view of MGC-neuron responses). In response to the same stimulus—10 ng of Z7-12:Ac—the maximum frequency measured on the PSTH was 2.4 times higher in MGC neurons (~120 AP/s) than in ORNs (~50 AP/s). When comparing the normalized response profiles of ORNs and MGC neurons (Figure 1C), the 2 signals are superimposed during the excitatory phase of MGC neurons but the inhibitory phase is only observed for MGC neurons and not for ORNs.

ORNs are strictly selective

Ninety-nine of 101 sensilla were tested with 100 ng of 3 pheromone compounds of the *A. ipsilon* female blend. Whereas 70% of the MGC neurons responded to hexane, none of the sensillar recordings presented responses to this control stimulation. Ninety-four ORNs responded only to Z7-12:Ac, 3 only to Z9-14:Ac, and 2 only to Z11-16:Ac. Such highly specific responses were also found in MGC neurons: 50% were specific for Z7-12:Ac, 16% specific for Z9-14:Ac, and 1% specific for Z11-16:Ac. However, some MGC neurons responded to 2 (12%) or 3 (20%) components (Figure 2).

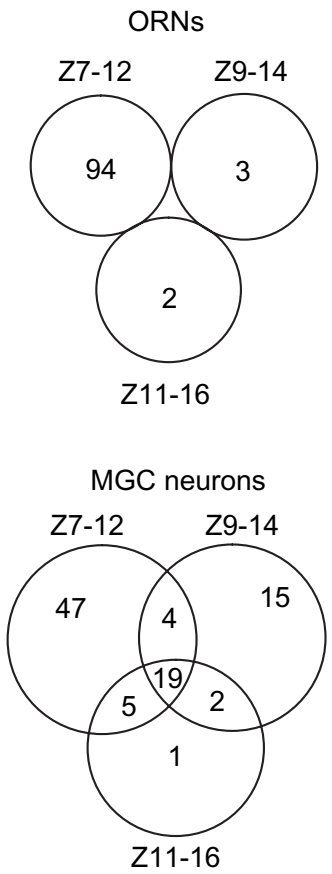

Figure 2 Distributions of the response specificity of 99 ORNs and 93 MGC neurons for the 3 components of the pheromone blend. ORNs were stimulated with 100 ng of each component and MGC neurons with 0.01 ng. ORNs were strictly selective regarding the 3 components, whereas 32% of the MGC neurons responded to more than one component. In both categories, most of the neurons responded to Z7-12:Ac.

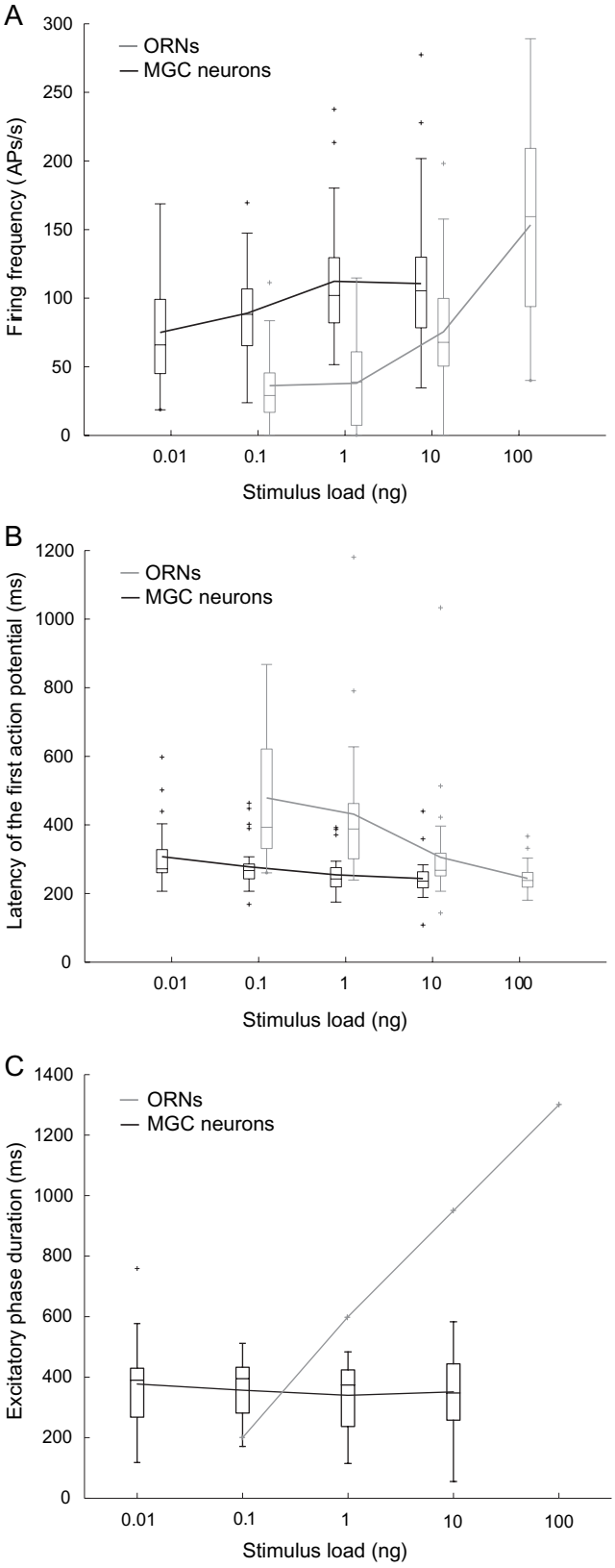

Threshold is more than 1000-fold higher in ORNs than in MGC neurons

The spontaneous activity preceding the stimulus was very low in ORNs compared with MGC neurons (0.34 ± 0.03 vs. 22.8 ± 1.55 APs/s). We considered that even a small change in the firing frequency of ORNs was sufficient to signal the presence of the pheromone. Thus, the response threshold was calculated as the lowest stimulus load eliciting a 5 APs/s increase of the firing frequency. Based on 45 ORNs tested with concentrations ranging from 0.1 to 100 ng, the response threshold was 1.5 ± 1.4 ng. The response threshold of MGC neurons was 0.005 ± 0.002 ng. Figure 3A shows that the firing frequency increases with the dose in both ORNs and MGC neurons (one-way ANOVA with repeated measures, ORNs: $F_{3,132} = 184.7$, $P < 0.001$; MGC neurons: $F_{3,84} = 11.5$, $P < 0.001$); it also shows that the firing frequency of MGC neurons reached its maximum at 10 ng, whereas at 100 ng the firing frequency of ORNs was still increasing. Moreover, the increase of firing frequency between 2 successive stimulus loads was higher for ORNs than for MGC neurons.

The latency of responses is more variable in ORNs than in MGC neurons

The latency of the first AP in the response decreased with increasing stimulus loads both in ORNs and MGC neurons (one-way repeated measures ANOVA, ORNs: unequal number of responding neurons; MGC neurons: $F_{3,84} = 14.2$, $P < 0.001$) (Figure 3B). For a same set of stimulus loads, the range of variation of this parameter is lower in MGC neurons (from 278 ± 13 ms at 0.1 ng to 244 ± 10 ms at 10 ng) than in ORNs (from 479 ± 62 ms at 0.1 ng to 310 ± 23 ms at 10 ng). Moreover, the variability across neurons represented by the interquartile range of the latencies is higher at low doses and higher in ORNs than in MGC neurons. The lowest values of latency for both ORNs and MGC neurons were measured at the highest dose tested and were similar (244 ± 10 ms for ORNs at 100 ng and 249 ± 7 ms for MGC neurons at 10 ng; Figure 3B).

Figure 3 Dose–response relationships for ORNs and MGC neurons in response to Z7-12:Ac. **(A)** Firing frequency: Increases in the firing frequency were detected for higher stimulus loads in ORNs (gray) than in MGC neurons (black). Although the firing frequency reached saturation at less than 10 ng in MGC neurons, no plateau is visible on the ORN dose–response curve. **(B)** Latency: The mean latencies of responses were higher for ORNs than for MGC neurons. At low stimulus loads, the variability was also higher for ORNs than for MGC neurons. **(C)** Duration: In ORNs, the response duration increases with the stimulus load, whereas in MGC neurons it does not. For ORNs, only the mean duration measured on PSTHs was plotted because the end of the response was difficult to determine in the recordings. On each plot, the box represents the interquartile range (IQR) of the data, the horizontal line inside the box represents the median, and the curve represents the mean. The whiskers show the range of the remaining sample. Outliers (+) are observations greater than 1.5 × IQR. For A and B the boxes and whiskers of ORNs and MGC neurons were slightly shifted to the left and right, respectively, to avoid their superimposition.

Encoding of stimulus load

Whereas the duration of the excitatory phase of MGC neurons was well defined by the inhibitory phase that followed (see response pattern in Figure 1), the response of ORNs was more difficult to delimit. The total duration of the tonic part of the response in ORNs could not be measured appropriately at high doses (100 and 10 ng) because the time needed for ORNs to return to their basal activity exceeded 15 s, which was the duration of poststimulus recordings. Instead of the actual response duration, we determined the time needed for the ORN firing frequency to decrease below 10% of the maximum reached during the response. This time increased with the stimulus load from 0.2 s at 0.1 ng to 1.3 s at 100 ng (Figure 3C). In MGC neurons, the duration of the response did not vary significantly with increasing stimulus loads as the duration of the excitatory and inhibitory phases were found to be independent of the stimulus load (see Figure 3C).

To understand which parameter within the ORN response might be read out by MGC neurons and thus influences the duration of the excitatory phase in the MGC-neuron response, we measured the relative response (as percentage of maximal response) of ORNs occurring at the same time as the end of the excitatory phase of MGC neurons. Because the duration of the excitatory phase of MGC neurons was independent of stimulus load (Jarriault et al. 2009), we first used the duration of the excitatory phase of 29 AL neurons averaged across 4 stimulus loads (0.01, 0.1, 1, and 10 ng) to determine the mean time at which MGC neurons ceased to fire when stimulated during 200 ms (T_{MGC}); we found T_{MGC} = 618 ± 15 ms after stimulus onset (horizontal black bar in Figure 4). Then we measured the relative response (as percentage of maximal response) of ORNs at this time (Figure 4). For the 3 highest stimulus loads (the PSTH for 0.1 ng was too variable for measuring the relative response reliably), we found that ORNs were firing at approximately one-third of the maximum firing frequency (30%, 30%, and 27% for 1, 10 and 100 ng, respectively; Figure 4).

Encoding of the stimulus duration in ORNs and MGC neurons

We compared the duration of the excitatory phase with increasing stimulus durations in ORNs (42 neurons) and MGC neurons (17 neurons). Whereas the response duration of ORNs increases with both the stimulus load (Figure 3C) and the stimulus duration (Table 1), we showed previously (Jarriault et al. 2009) that the duration of the excitatory phase of MGC neurons was independent of the stimulus load but increased proportionally to the stimulus duration. Using the same method as above, we examined the relative firing activity of ORNs (as percentage of maximal firing) when MGC neurons ceased to fire in response to stimuli of different durations. Lower stimulus loads were used for MGC

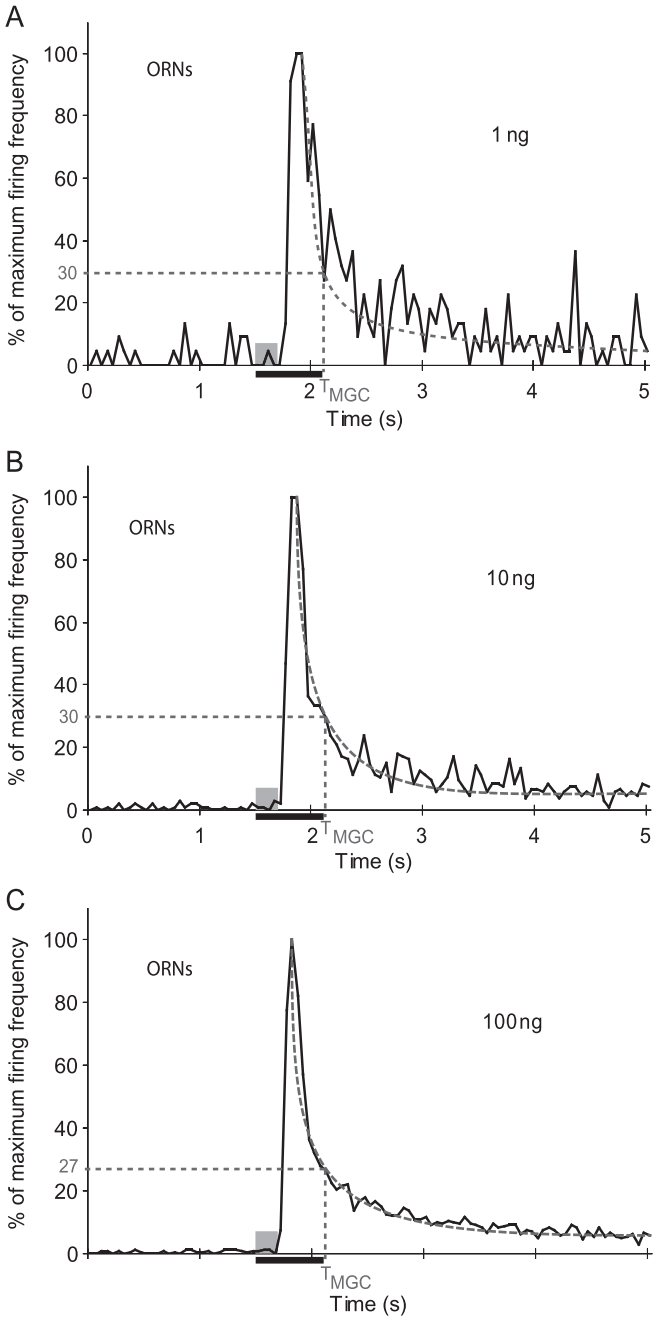

Figure 4 Relative responses of ORNs as a function of time, when stimulated with different stimulus loads. **(A–C)** PSTHs of ORNs were normalized with respect to the maximum firing frequency of the response (as in Figure 1C) at 3 stimulus loads (1, 10, 100 ng) of Z7-12:Ac. Gray bars represent the stimulation period. The response duration in MGC neurons did not vary with the stimulus load (horizontal black bar) so that the times at which the 29 investigated MGC neurons stopped to fire in response to the stimulus were averaged across the 3 stimulus loads. This unique time value T_{MGC} (618 ± 15 ms) was used to determine the percentage of ORN spiking activity when MGC neurons stopped to fire. On average, at T_{MGC}, the ORN firing frequency was determined as about 30% of its maximum on smoothed curves (hatched lines).

neurons (from 0.01 to 1 ng) because of their higher sensitivity compared with ORNs. The time at which MGC neurons ceased to fire (Table 1) was always shorter than the ORN response duration. Then, we measured the firing frequency of ORNs at the time at which MGC neurons stopped to fire (durations of their excitatory phase are represented by the horizontal black bars in Figure 5) and we expressed it in percentage of its maximum on the normalized PSTHs. For the 4 tested stimulus durations, we found that the ORN firing frequency was respectively 23%, 25%, 31%, and 27% of its maximum (see Table 1).

Discussion

We analyzed the input and output of the AL of the moth *A. ipsilon* by stimulating the male antenna with 3 sex pheromone components tested at various doses and different stimulus durations. The same protocol of stimulation was used when recording from ORNs or MGC neurons. Comparison of the responses of ORNs and MGC neurons showed both similarities and striking differences, thus revealing the transformation of the pheromonal antennal code at this first level of central processing. As reported in Jarriault et al. (2009) the uniformity of the MGC-neuron responses

Table 1 Termination of the excitatory phase in MGC neurons and relative response of ORNs at different stimulus durations

Stimulus duration	100 ms (T_{100})	200 ms (T_{200})	500 ms (T_{500})	1000 ms (T_{1000})
ORN response duration (ms)[a]	700	900	2150	3000
Time at which PNs ceased to fire after stimulus onset (ms)	470 ± 5	480 ± 4	720 ± 10	1210 ± 26
Percentage of the maximum spike frequency in ORNs	23	25	31	27

[a]Calculated as the time during which the relative spike frequency was above 10% of its maximum (as described in the Materials and methods).

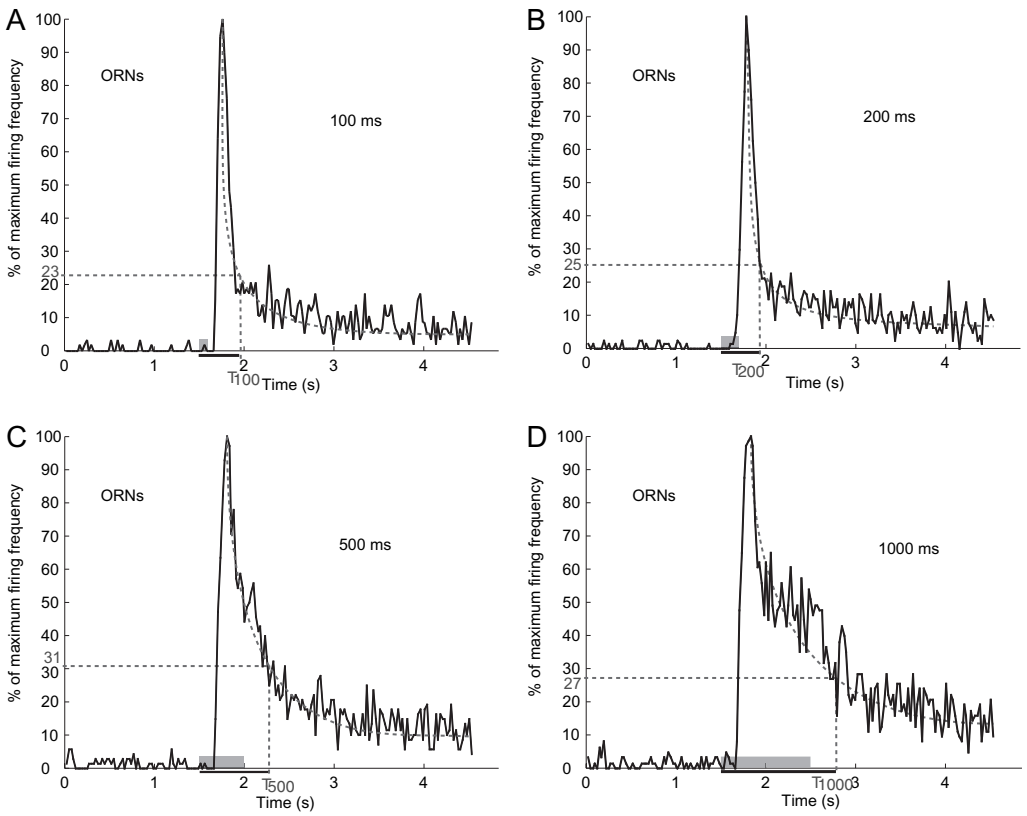

Figure 5 Relative responses of ORNs as a function of time, when stimulated with Z7-12:Ac at different durations. **(A–D)** The response profile of ORNs is represented by a PSTH for each stimulus duration (stimulus load 10 ng). Gray bars represent the stimulation period. MGC neurons were shown to increase the duration of their excitatory phase linearly with increasing stimulus durations. Horizontal black bars and T_{100}, T_{200}, T_{500}, and T_{1000} are, respectively, the durations of MGC-neuron excitatory phase and the times at which they stopped to fire in response to these stimulus durations. On average, the ORN firing frequency was determined as about 30% of its maximum on smoothed curves (hatched lines) at these different times.

(biphasic pattern) and their characteristic morphology when stained (cell body in the medial cell cluster and axon leaving the AL via the inner antenno-cerebral tract) indicate strongly that they are PNs.

High correlation between ORN and MGC-neuron signals during the excitatory phase of the MGC-neuron response

Most MGC neurons showed a sustained spontaneous activity, which was not observed in the ORNs. Both ORNs and MGC neurons showed similar temporal profiles during the early response phase corresponding to the excitatory phase in MGC neurons: both neuron types responded with a phasic–tonic pattern and the time courses of their normalized firing frequencies were superimposed (Figure 1C). This might suggest that the excitatory phase of the MGC neurons in response to pheromone components originates from direct synaptic input from ORNs. Anatomical studies supporting direct synaptic contacts between these 2 neuron types were shown by electron microscopy in several insect species such as *Periplaneta americana* (Distler and Boeckh 1996) and *Drosophila* sp. (Stocker 1994). However, other types of transmission such as disinhibition via a network of LNs could elicit the same type of response pattern (Christensen et al. 1993). Synaptic connections between ORNs and LNs and between LNs and PNs have been described anatomically (Tolbert and Hildebrand 1981; Distler 1990; Distler and Boeckh 1997), which indicate that such a network might indeed exist.

The present results also showed that ORN response latencies were highly variable, suggesting that activated ORNs do not send signals to the MGC simultaneously. The same observation was reported in *Drosophila* (Bhandawat et al. 2007). However, normalized ORN and MGC-neuron PSTHs were superimposed, suggesting the following. First, the delay between the first AP produced in response to pheromone stimulation by the ORNs and by the MGC neurons is very short. Second, in the PSTHs, the time at which the ORN activity starts to increase, which is indicative of the latency of the ORN population, is similar to the response latency of the MGC-neuron population. Controversial observations were published regarding this topic: in the fruitfly, the rise in firing frequency occurs later in ORNs than in PNs for the sampled neurons (Wilson et al. 2004; Bhandawat et al. 2007), whereas in the honeybee, PNs responded at least 60 ms after an input in the AL (Krofczik et al. 2009). In our case, MGC neurons may initiate response upon arrival of the earliest ORN input.

Inhibitory phase in MGC neurons but not in ORNs: shaping of the signal by LNs

Although the signals in ORNs and MGC neurons were very similar during the excitatory phase of MGC neurons, they diverged afterward. The response pattern of MGC neurons in our study with an excitatory phase, followed by an inhibitory phase has been described as typical for PNs in *A. ipsilon* (Gadenne and Anton 2000; Jarriault et al. 2009), which is in agreement with responses observed in PNs of other invertebrate species (*Manduca sexta*: Matsumoto and Hildebrand 1981; lobster: Wachowiak and Ache 1994; *Drosophila melanogaster*: Wilson et al. 2004) and in mitral/tufted cells of vertebrates (Hamilton and Kauer 1989; Nakanishi 1995). In all studies on MGC neurons in *A. ipsilon*, we so far never encountered an LN with this response pattern (Jarriault D., personal observation). The inhibitory phase constitutes the most striking part of the transformation occurring between input and output of the AL. It is suppressed in pharmacological experiments blocking the action of AL/OB GABAergic interneurons, which favors the hypothesis that LNs play a role in shaping the inhibitory phase of PN/mitral/tufted cell responses (Waldrop et al. 1987; Christensen et al. 1993, 1998; Shipley and Ennis 1996; Friedrich and Laurent 2001, 2004; Wachowiak et al. 2005; Wilson and Laurent 2005; Pírez and Wachowiak 2008; Lei et al. 2009).

Convergence increases the MGC-neurons sensitivity but imposes a gain control

Not all ORNs responded in the same way and thus transmitted the same information to the MGC. ORNs showed a large variability in their response threshold and in their firing rate in response to a given stimulus load. No threshold in our ORN sample was as low as the threshold of MGC neurons, which indicates that this sample (45 neurons) was not large enough to include the rare ORNs with very low thresholds. Data on the olfactory system of mice suggest, however, that the filtering system in early olfactory circuits favors the input from the most sensitive ORNs (Hamana et al. 2003).

A 1000-fold increase in sensitivity was observed when comparing the response thresholds of ORNs and MGC neurons. Such a shift in the dose–response curves and response thresholds was reported for other insects (Boeckh 1974; Boeckh and Selsam 1984; Boeckh and Ernst 1987; Hansson et al. 1991; Christensen and Hildebrand 1994; Hartlieb et al. 1997). It reflects the convergence of a high number of ORNs onto fewer MGC neurons, a ratio, which is larger in the sex pheromone system than in the plant odor system (Boeckh and Ernst 1987; Stocker 1994; Root et al. 2007). Moreover, the firing frequency in MGC neurons reaches saturation at a lower dose than in ORNs. Therefore, at high concentration, the message sent by ORNs into the MGC might not be transmitted to the subsequent step of integration in the protocerebrum. As LNs have been proposed to control the gain of the input to the AL (Olsen et al. 2007; Olsen and Wilson 2008), they could act in this process to limit the ORN input on the MGC neurons.

Broader tuning of MGC neurons

No ORNs were found to respond to more than one of the 3 tested components. On the contrary, a non-negligible number of MGC neurons responded to 2 or all 3 components. As each ORN type is thought to project to a unique

glomerulus (Hansson et al. 1992; Christensen et al. 1995a; Ochieng et al. 1995; Todd et al. 1995; Lee et al. 2006a,b; Karpati et al. 2008), PNs responding to more than one component are thought either to arborize in more than one glomerulus or to receive inputs from other glomeruli via LNs. Both hypotheses are corroborated by anatomical results in *A. ipsilon* and in other species. Some intracellularly stained PNs and LNs arborizing in several glomeruli of the MGC were found (Matsumoto and Hildebrand 1981; Hansson et al. 1994; Jarriault D., personal observation). The mismatching between axonal projections of ORNs and dendritic arborizations of PNs responding to the same pheromone component was also studied in *Trichoplusia ni* (Anton and Hansson 1999). Less than 70% of the analyzed PNs showed dendrites overlapping with the terminals of ORNs displaying identical specificities, which underlines that LNs play a role in distributing information among glomeruli (Anton and Hansson 1999). A clear difference between ORNs and PNs has also been found in the capacity to encode specific pheromone blends. Whereas ORNs respond primarily to pheromone blends containing the component they are tuned to (e.g., Carlsson and Hansson 2002), blend-specific PNs have been described in different moth species (e.g., Christensen et al. 1995b; Wu et al. 1996; Anton et al. 1997). In addition to the broader tuning of MGC neurons, differences in the proportions of neurons responding to each pheromone component were observed: 94% of the studied ORNs versus 80% of the PNs responded to Z7-12:Ac, 3% of the ORNs versus 43% of the PNs responded to Z9-14:Ac, and 2% of the ORNs versus 29% of the PNs responded to Z11-16:Ac. Although the predominance of the major component, Z7-12:Ac, in the distribution was clearly conserved at both levels, the 2 other components elicited much more responses in MGC neurons than in ORNs. Although we cannot exclude a bias in our ORN sampling, our results suggest that information on minor pheromone components is reinforced at the level of the MGC as compared with the sensory input.

The relative level of ORN firing could determine the end of the MGC-neuron excitatory phase

The relative response of ORNs at different doses (Figure 4) and different stimulus durations (Figure 5) at the mean time at which MGC neurons ceased to fire (T_{MGC}) showed consistent results, that is, the termination of the excitatory phase of the PN response depends on the relative level of the ORN firing frequency. To explain the independence of the MGC-neuron response duration from the stimulus load, we propose that a mechanism in the AL terminates the MGC-neuron response when the ORN input decreases below a certain level, the value of which depends on the stimulus load. When MGC neurons ceased to fire, ORNs fired at approximately 30% of their maximum (firing frequency which is reached during the response). This was observed for 3 logarithmic steps of stimulus loads. When testing the relevance of this threshold value for the duration of the excitatory phase of the MGC neurons, we observed that the same relative level of activity applied in ORNs. This activity level–based mechanism might result from the relative strength of excitatory and inhibitory inputs in the MGC. Based on the previous studies showing an involvement of LNs in the termination of the MGC-neuron signal (discussed above), we propose that LN activity might be sensitive to (or be driven by) a certain level of ORN input. The proposed mechanism would therefore be concentration independent and would rely only on the stimulus duration.

Conclusions

Our input–output analysis of the pheromone-induced responses confirmed that the incoming message from the ORNs is profoundly reshaped in the MGC circuits and that the sensitivity of MGC neurons is much higher than that of ORNs; the later property imposes a gain control to limit the saturation of the encoding capacity of MGC neurons at high doses. We show that MGC-neuron responses are precisely correlated to stimulus durations; we suggest that this correlation could result from an inhibitory input provided by the LNs based on the ORN input intensity. Further experiments exploring the intrinsic properties of AL neurons will help to document the role of LNs in the effects reported here. Beyond their contribution to the analysis of the neural mechanisms involved in olfactory coding sensu stricto, the present results will also serve to better understand the mechanisms that lead to the plasticity of pheromone-guided behavior, which seems to originate from changes in the sensitivity of neurons within the AL of *A. ipsilon* (Anton et al. 2007).

Funding

This work was supported by a PhD grant to D.J. from Pierre and Marie Curie University; "Projet Jeune Equipe" INRA grant to C.G. and S.A.; French–British Grant Agence Nationale de la Recherche – Biotechnology and Biological Sciences Research Council (ANR-BBSRC) Sysbio 006 01 "Pherosys" to J.-P.R., S.A., and P.L.

Acknowledgements

We thank C. Chauvet and C. Gaertner for their help with insect rearing, and Dr Hong Lei and anonymous referees for helpful comments on a previous version of the manuscript.

References

Anton S, Dufour MC, Gadenne C. 2007. Plasticity of olfactory-guided behaviour and its neurobiological basis: lessons from moths and locusts. Ent Exp Appl. 123:1–11.

Anton S, Hansson B. 1999. Physiological mismatching between neurons innervating olfactory glomeruli in a moth. Proc R Soc B Biol Sci. 266:1813–1820.

Anton S, Homberg U. 1999. Antennal lobe structure. In: Hansson BS, editor. Insect olfaction. Berlin: Springer. p. 98–125.

Anton S, Löfstedt C, Hansson B. 1997. Central nervous processing of sex pheromones in two strains of the European corn borer *Ostrinia nubilalis* (*Lepidoptera: pyralidae*). J Exp Biol. 200:1073–1087.

Berg BG, Almaas TJ, Bjaalie JG, Mustaparta H. 1998. The macroglomerular complex of the antennal lobe in the tobacco budworm moth *Heliothis virescens*: specified subdivision in four compartments according to information about biologically significant compounds. J Comp Physiol A. 183:669–682.

Bhandawat V, Olsen SR, Schlief ML, Gouwens NW, Wilson RI. 2007. Sensory processing in the *Drosophila* antennal lobe increases the reliability and separability of ensemble odor representations. Nat Neurosci. 10:1474–1482.

Boeckh J. 1974. Reactions of olfactory neurons in the insect deutocerebrum as compared to response patterns of olfactory receptor cells. J Comp Physiol A. 90:183–205.

Boeckh J, Ernst KD. 1987. Contribution of single unit analysis in insects to an understanding of olfactory function. J Comp Physiol A. 161:549–565.

Boeckh J, Selsam P. 1984. Quantitative investigation of the odour specificity of central olfactory neurones in the American cockroach. Chem Senses. 9:369–380.

Buck LB, Axel R. 1991. A novel multigene family may encode odorant receptors: a molecular basis for odor recognition. Cell. 65:175–187.

Buck LB. 1996. Information coding in the vertebrate olfactory system. Annu Rev Neurosci. 19:517–544.

Carlsson MA, Hansson BS. 2002. Responses in highly selective sensory neurons to blends of pheromone components in the moth *Agrotis segetum*. J Insect Physiol. 48:443–451.

Causse R, Buès R, Barthes J, Toubon J. 1988. Mise en évidence expérimentale de nouveaux constituants des phéromones sexuelles de *Scotia ipsilon* et *Mamestra suasa*. In: INRA, editor. Médiateurs chimiques: comportement et systématique des lépidoptères. Coll. INRA n 46. Paris (France): INRA. p. 75–82.

Christensen TA, Harrow ID, Cuzzocrea C, Randolph PW, Hildebrand JG. 1995a. Distinct projections of two populations of olfactory receptor axons in the antennal lobe of the sphinx moth *Manduca sexta*. Chem Senses. 20:313–323.

Christensen TA, Hildebrand JG. 1987. Male-specific, sex pheromone-selective projection neurons in the antennal lobes of the moth, *Manduca sexta*. J Comp Physiol A. 160:553–569.

Christensen TA, Hildebrand JG. 1994. Neuroethology of sexual attraction and inhibition in heliothine moths. Neural basis of behavioural adaptations. Prog Zool. 39:37–46.

Christensen T, Mustaparta H, Hildebrand JG. 1995b. Chemical communication in heliothine moths. VI: parallel pathways for information processing in the macroglomerular complex of the male tobacco budworm moth *Heliothis virescens*. J Comp Physiol A. 177:545–557.

Christensen TA, Waldrop BR, Harrow ID, Hildebrand JG. 1993. Local interneurons and information processing in the olfactory glomeruli of the moth *Manduca sexta*. J Comp Physiol A. 173:385–399.

Christensen TA, Waldrop BR, Hildebrand JG. 1998. GABAergic mechanisms that shape the temporal response to odors in moth olfactory projection neurons. Ann N Y Acad Sci. 855:475–481.

Clyne P, Grant A, O'Connell R, Carlson JR. 1997. Odorant response of individual sensilla on the *Drosophila* antenna. Invert Neurosci. 3: 127–135.

Distler P. 1990. GABA-immunohistochemistry as a label for identifying types of local interneurons and their synaptic contacts in the antennal lobes of the American cockroach. Histochem Cell Biol. 93:617–626.

Distler PG, Boeckh J. 1996. Synaptic connection between olfactory receptor cells and uniglomerular projection neurons in the antennal lobe of the American cockroach, *Periplaneta americana*. J Comp Neurol. 370:35–46.

Distler PG, Boeckh J. 1997. Synaptic connections between identified neuron types in the antennal lobe glomeruli of the cockroach, *Periplaneta americana*: I. Uniglomerular projection neurons. J Comp Neurol. 378:307–319.

Dolzer J, Fischer K, Stengl M. 2003. Adaptation in pheromone-sensitive trichoid sensilla of the hawkmoth *Manduca sexta*. J Exp Biol. 206: 1575–1588.

Friedrich RW, Laurent G. 2001. Dynamic optimization of odor representations by slow temporal patterning of mitral cell activity. Science. 291: 889–894.

Friedrich RW, Laurent G. 2004. Dynamics of olfactory bulb input and output activity during odor stimulation in zebrafish. J Neurophysiol. 91: 2658–2669.

Gadenne C, Anton S. 2000. Central processing of sex pheromone stimuli is differentially regulated by juvenile hormone in a male moth. J Insect Physiol. 46:1195–1206.

Gao Q, Yuan B, Chess A. 2000. Convergent projections of *Drosophila* olfactory neurons to specific glomeruli in the antennal lobe. Nat Neurosci. 3:780–785.

Gemeno C, Haynes KF. 1998. Chemical and behavioral evidence for a third pheromone component in a North American population of the black cutworm moth, *Agrotis ipsilon*. J Chem Ecol. 24:999–1011.

Hamana H, Hirono J, Kizumi M, Sato T. 2003. Sensitivity-dependent hierarchical receptor codes for odors. Chem Senses. 28:87–104.

Hamilton KA, Kauer JS. 1989. Patterns of intracellular potentials in salamander mitral/tufted cells in response to odor stimulation. J Neurophysiol. 62:609–625.

Hansson BS, Anton S, Christensen TA. 1994. Structure and function of antennal lobe neurons in the male turnip moth, *Agrotis segetum* (Lepidoptera: Noctuidae). J Comp Physiol A. 175:547–562.

Hansson BS, Christensen TA, Hildebrand JG. 1991. Functionally distinct subdivisions of the macroglomerular complex in the antennal lobe of the male sphinx moth *Manduca sexta*. J Comp Physiol A. 312:264–278.

Hansson BS, Christensen TA. 1999. Functional characteristics of the antennal lobe. In: Hansson BS, editor. Insect olfaction. Berlin (Germany): Springer-Verlag. p. 125–161.

Hansson BS, Ljungberg H, Hallberg E, Lofstedt C. 1992. Functional specialization of olfactory glomeruli in a moth. Science. 256:1313–1315.

Hartlieb E, Anton S, Hansson BS. 1997. Dose-dependent response characteristics of antennal lobe neurons in the male moth *Agrotis segetum* (Lepidoptera: Noctuidae). J Comp Physiol A. 181:469–476.

Homberg U, Christensen TA, Hildebrand JG. 1989. Structure and function of the deutocerebrum in insects. Annu Rev Entomol. 34:477–501.

Jarriault D, Gadenne C, Rospars JP, Anton S. 2009. Quantitative analysis of sex-pheromone coding in the antennal lobe of the moth *Agrotis ipsilon*: a tool to study network plasticity. J Exp Biol. 212:1191–1201.

Kaissling KE, Thorson J. 1980. Insect olfactory sensilla: structural, chemical and electrical aspects of the functional organization. In: Sattelle DB, Hall LM, Hildebrand JG, editors. Receptors for transmitters, hormones and pheromones in insects. Amsterdam (The Netherlands): Elsevier. p. 261–282.

Karpati Z, Dekker T, Hansson BS. 2008. Reversed functional topology in the antennal lobe of the male European corn borer. J Exp Biol. 211: 2841–2848.

Koontz MA, Schneider D. 1987. Sexual dimorphism in neuronal projections from the antennae of silk moths (*Bombyx mori, Antheraea polyphemus*) and the gypsy moth (*Lymantria dispar*). Cell Tissue Res. 249:39–50.

Krieger J, Raming K, Dewer YME, Bette S, Conzelmann S, Breer H. 2002. A divergent gene family encoding candidate olfactory receptors of the moth *Heliothis virescens*. Eur J Neurosci. 16:619–628.

Krofczik S, Menzel R, Nawrot MP. 2009. Rapid odor processing in the honeybee antennal lobe network. Front Comput Neurosci. 2:9.

Lee SG, Carlsson MA, Hansson BS, Todd JL, Baker TC. 2006. Antennal lobe projection destinations of *Helicoverpa zea* male olfactory receptor neurons responsive to heliothine sex pheromone components. J Comp Physiol A. 192:351–363.

Lee SG, Vickers NJ, Baker TC. 2006. Glomerular targets of *Heliothis subflexa* male olfactory receptor neurons housed within long trichoid sensilla. Chem Senses. 31:821–834.

Lei H, Riffell JA, Gage SL, Hildebrand JG. 2009. Contrast enhancement of stimulus intermittency in a primary olfactory network and its behavioral significance. J Biol. 8:21.

Malun D. 1991. Synaptic relationships between GABA-immunoreactive neurons and an identified uniglomerular PN in the antennal lobe of *Periplaneta americana*: a double-labeling electron microscopic study. Histochem. 96:197–207.

Matsumoto SG, Hildebrand JG. 1981. Olfactory mechanisms in the moth *Manduca sexta*: response characteristics and morphology of central neurons in the antennal lobes. Proc R Soc B Biol Sci. 213:249–277.

Mori K. 1998. Chirality and insect pheromones. Chirality. 10:578–586.

Nakanishi S. 1995. Second-order neurones and receptor mechanisms in visual-and olfactory-information processing. Trends Neurosci. 18:359–364.

Ochieng SA, Anderson P, Hansson BS. 1995. Antennal lobe projection patterns of olfactory receptor neurons involved in sex pheromone detection in *Spodoptera littoralis* (Lepidoptera: Noctuidae). Tissue Cell. 27:221–232.

Olsen SR, Bhandawat V, Wilson RI. 2007. Excitatory interactions between olfactory processing channels in the *Drosophila* antennal lobe. Neuron. 54:89–103.

Olsen SR, Wilson RI. 2008. Lateral presynaptic inhibition mediates gain control in an olfactory circuit. Nature. 452:956–962.

Picimbon JF, Gadenne C, Bécard JM, Clément JL, Sreng L. 1997. Sex pheromone of the French black cutworm moth, *Agrotis ipsilon* (Lepidoptera: Noctuidae): identification and regulation of a multicomponent blend. J Chem Ecol. 23:211–230.

Pírez N, Wachowiak M. 2008. In vivo modulation of sensory input to the olfactory bulb by tonic and activity-dependent presynaptic inhibition of receptor neurons. J Neurosci. 28:6360–6371.

Poitout S, Buès R. 1974. Elevage de plusieurs espèces de lépidoptères sur milieu artificiel simplifié. Ann Zool Ecol Anim. 2:79–91.

Renou M, Gadenne C, Tauban D. 1996. Electrophysiological investigations of pheromone-sensitive sensilla in the hybrids between two moth species. J Insect Physiol. 42:267–277.

Root CM, Semmelhack JL, Wong AM, Flores J, Wang JW. 2007. Propagation of olfactory information in *Drosophila*. Proc Nat Acad Sci U S A. 104:11826–11831.

Rospars JP. 1988. Structure and development of the insect antennodeutocerebral system. Int J Insect Morphol Embryol. 17:243–294.

Sakurai T, Nakagawa T, Mitsuno H, Mori H, Endo Y, Tanoue S, Yasukochi Y, Touhara K, Nishioka T. 2004. Identification and functional characterization of a sex pheromone receptor in the silkmoth *Bombyx mori*. Proc Nat Acad Sci U S A. 101:16653–16658.

Shipley MT, Ennis M. 1996. Functional organization of olfactory system. J Neurobiol. 30:123–176.

Stocker RF. 1994. The organization of the chemosensory system in *Drosophila melanogaster*: a review. Cell Tissue Res. 275:3–26.

Todd JL, Anton S, Hansson BS, Baker TC. 1995. Functional organization of the macroglomerular complex related to behaviourally expressed olfactory redundancy in male cabbage looper moths. Physiol Entomol. 20:349–361.

Tolbert LP, Hildebrand JG. 1981. Organization and synaptic ultrastructure of glomeruli in the antennal lobes of the moth *Manduca sexta*: a study using thin sections and freeze-fracture. Proc R Soc B Biol Sci. 213: 279–301.

Vosshall LB, Amrein H, Morozov PS, Rzhetsky A, Axel R. 1999. A spatial map of olfactory receptor expression in the *Drosophila* antenna. Cell. 96: 725–736.

Vosshall LB, Wong AM, Axel R. 2000. An olfactory sensory map in the fly brain. Cell. 102:147–159.

Wachowiak M, Ache BW. 1994. Morphology and physiology of multiglomerular olfactory projection neurons in the spiny lobster. J Comp Physiol A. 175:35–38.

Wachowiak M, McGann JP, Heyward PM, Shao Z, Puche AC, Shipley MT. 2005. Inhibition of olfactory receptor neuron input to olfactory bulb glomeruli mediated by suppression of presynaptic calcium influx. J Neurophysiol. 94:2700–2712.

Wakamura S, Struble DL, Matsuura H, Sato M, Kegasawa K. 1986. Sex pheromone of the black cutworm, *Agrotis ipsilon*: attractant synergist and improved formulation. Appl Entomol Zool. 21:299–304.

Waldrop B, Christensen TA, Hildebrand JG. 1987. GABA-mediated synaptic inhibition of projection neurons in the antennal lobes of the sphinx moth *Manduca sexta*. J Comp Physiol A. 161:23–32.

Wilson R, Laurent G. 2005. Role of GABAergic inhibition in shaping odor-evoked spatiotemporal patterns in the *Drosophila* antennal lobe. J Neurosci. 25:9069–9079.

Wilson RI, Turner GC, Laurent G. 2004. Transformation of olfactory representations in the *Drosophila* antennal lobe. Science. 303: 366–370.

Wu W, Anton S, Löfstedt C, Hansson BS. 1996. Discrimination among pheromone component blends by interneurons in male antennal lobes of two populations of the turnip moth, *Agrotis segetum*. Proc Nat Acad Sci U S A. 93:8022–8027.